Journal of Structural Geology, Vol. 12, No. 2, pp. 145 to 164, 1990
Printed in Great Britain

0191-8141/90 $03.00 + 0.00

Origin of kinkbands and shear-band cleavage in shear zones: an experimental study

P. F. WILLIAMS

Department of Geology, University of New Brunswick, Fredericton, N.B., Canada E3B 5A3

and

G. P. PRICE

Division of Geomechanics, CSIRO, P.O. Box 54, Mt. Waverley, Victoria 3149, Australia

(*Received* 31 *August* 1988; *accepted in revised form* 26 *June* 1989)

Abstract—Specimens of artificial KCl–mica schist have been deformed in simple shear with different initial orientations (10° intervals between 0° and 170°) of the mica schistosity (S_1) relative to the imposed simple-shear plane. For most experiments the angular shear strain was 30°, the strain rate $4.8 \times 10^{-4}\,s^{-1}$ and the stress normal to the imposed shear plane 20 MPa. All experiments were conducted at room temperature.

Deformation of the specimens is achieved largely by slip parallel to the S_1 mica foliation. However, two new types of slip surfaces also develop, as either a single orientation set or as a pair of conjugate sets. These new slip surfaces are kinkbands and a shear-band cleavage. The type and number of sets of new slip surfaces which develop depends on the orientation of S_1 relative to the shortening and extension fields of the instantaneous strain ellipsoid.

Our experiments indicate that kinkbands or shear-band cleavage form in shear zones in which S_1 is inclined to the margin of the zone. Which structure forms and whether it occurs as a single set of structures or as a conjugate pair depends on the initial orientation of S_1. In situations where S_1 is parallel to the margins of the zone neither structure develops if the deformation is a simple shear. The presence of kinkbands or shear-band cleavage in such zones, where S_1 is parallel to the margins, is an indication that the zones were transtensional or transpressional, respectively.

We conclude that shear-band cleavage is not only an excellent indicator of shear sense but also a qualitative indicator of the ratio of S_1-normal shortening to S_1-parallel shear. Conjugate shear bands indicate that S_1-normal shortening was relatively strong and single shear-band sets indicate that S_1-parallel shear was relatively strong.

INTRODUCTION

THERE has been considerable interest in recent years in shear zones, in the structures developed within them and in the more general problem of progressive strain (e.g. Ramsay & Graham 1970, Williams & Zwart 1977, Berthé *et al.* 1979, Lister & Williams 1983, Cobbold *et al.* 1987). In this paper we report on a series of experiments designed to simulate the structures and microstructures developed in such zones in response to a progressive simple shear. The structures developed (Fig. 1) include symmetrical folds, kinkbands and a shear-band type crenulation cleavage (White *et al.* 1980).

The experiments were performed in a simple-shear deformation rig designed by Price (Price & Torok 1989). The rig constrains an approximately $58 \times 47 \times 48$ mm rectangular prism of rock or analogue material (Fig. 1a) to undergo a simple-shear–strain history up to an angular shear strain of 30° (Fig. 2), which gives a shortening of 25%. The specimen is deformed in a Teflon-lined steel chamber and there is a slight departure from ideal simple shearing of the external boundaries of the block due to deformation and redistribution of the thin (up to 1 mm thick) Teflon lining. Further small departures from ideal simple shearing can result from compaction of the specimen and from slight rotation of the lower surface of the chamber about the intermediate strain axis (Figs. 2b & c). Experiments are performed at room temperature and confining pressure is achieved by loading the specimen perpendicular to the horizontal shear plane prior to shearing. Normal loads in the range 0–80 MPa are routinely attainable. Strain rate, in terms of rate of angular shear, can be varied from a maximum of $1.0\,deg\,s^{-1}$ to rates determined, in practical terms, only by the time available. For the total 25% shortening the maximum average shortening rate is $8.3 \times 10^{-3}\,s^{-1}$.

Various materials including marble and phyllite have been deformed in the ductile field (Price & Torok 1989) but the most interesting microstructures are obtained in artificial 'schists' composed of NaCl and mica or KCl and mica. The best shear-band cleavage (S_2) develops in wet NaCl–mica specimens deformed at slow strain rates; however, only slightly inferior shear-band cleavage is obtained in dry KCl–mica specimens at faster strain rates and our efforts have therefore been concentrated on this material. In this paper we are concerned primarily with a series of experiments on KCl–mica 'schist' in which the only experimental variable was the orientation of the primary schistosity (S_1).

In experiments of this kind there is always the concern that the results may be due solely to artificial boundary conditions and therefore not relevant to natural situations. Our assumption, which is supported by the distribution of deformation microstructures in the speci-

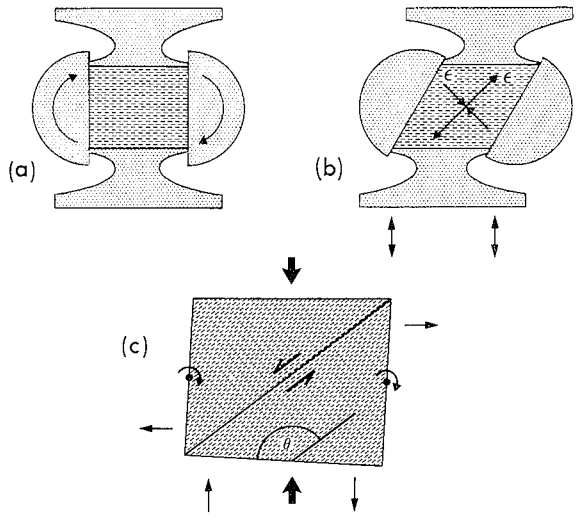

Fig. 2. Diagrammatic representation of specimen and deformation chamber. (a) Shows the initial configuration—arrows indicate the sense of rotation of the half cylinders that drive the deformation. (b) Shows the deformed configuration and the instantaneous strain axes. The arrows below the figure indicate the possible limited vertical movements of the lower platen. (c) Indicates the rotation of the half cylinders and the vertical movements of the lower platen that result from interaction of the inclined S_1 and the normal load. The half arrows indicate the sense of shear on S_1.

men, is that the specimens are sufficiently large that constraints in their centres approximate the natural constraints found in a body of rock undergoing a progressive simple shear. Our confidence in this assumption is also supported by a series of numerical modelling experiments designed to simulate the plane-strain physical experiments. The modelling experiments were carried out using a code capable of simulating a single slip-system material. Various aspect ratios and array sizes were used to assess the effects of the closeness of the boundaries. The resulting structures, which are essentially the same as those produced in the corresponding physical experiments, indicate that the size and shape of the physical specimens are not significant factors. The numerical work is continuing and will be reported at a later date.

In the following description and discussion we refer to the orientations of various planar structures. All such structures contain a line approximately normal to the simple-shear vector lying in the shear plane (i.e. the intermediate strain axis). The orientations are expressed as angles from 0° to 180° measured clockwise in the plane normal to the intermediate strain axis with 0° coinciding with the trace of the shear plane. All experiments are viewed such that the simple shearing is dextral.

SAMPLE PREPARATION

Cylindrical blocks of KCl–mica 'schist' were prepared by compacting a mixture of 70 wt % KCl and 30 wt % mica in a 100 mm diameter, cylindrical pellet-press. Particle size was between 0.15 and 0.5 mm for mica and <0.5 mm for KCl. The KCl was dried at 50°C for 24 h and then mixed with the mica. The mixture was sprinkled into the pellet-press to a depth of approximately 10 mm and was compacted at a nominal 40 MPa for 90 s to form one layer of the specimen. The upper surface of this compressed layer was then sprayed with a saturated solution of KCl and more layers of mixture were added and compacted in the same way until the cylindrical blocks were approximately 90 mm thick. Finally, the cylindrical blocks were further compacted at a nominal 40 MPa for 60 min and then dried at 50°C for a minimum of 24 h. The resultant cylindrical blocks, approximately 85 mm thick, are strongly foliated (Fig. 1b) and have weakly defined bedding planes due to a slight concentration of mica at the top of each layer (visible as horizontal fractures in Fig. 1c). We refer to the initial strong foliation as S_1. The cylindrical blocks also have a weakly developed conjugate pair of impersistent ductile shears that are symmetrical with respect to the foliation and have a sense of shear that is compatible with the foliation-normal compacting stress (Fig. 1b). The angle between the conjugate surfaces containing the shortening direction is approximately 80°.

Rectangular specimens, in various orientations relative to S_1 were cut from the cylinders (Fig. 1a) such that they would fit as close as possible to the dimensions of the deformation chamber. Allowance was made for a thin (<1 mm) layer of Teflon on the ends of the specimens, and two and three Teflon layers on the two vertical sides, respectively. The multiple layers on the sides facilitate removal of the specimens without breakage after deformation.

EXPERIMENTAL CONDITIONS

The main series of experiments (Table 1) was carried out using the KCl–mica mix at a strain rate of 5.6×10^{-4} deg s^{-1} angular shear which is equal to an average rate of shortening of 4.8×10^{-6} s^{-1}. The experiments were run dry, at room temperature, 20 MPa normal stress and were strained to an angular shear of 30°. The initial dip (θ) of S_1 (Fig. 2c) was varied in 10° steps from 0° to 170°. All specimens in which S_1 was dipping relative to the shear plane were cut such that the intersection of S_1 with the shear plane was perpendicular to the shear-movement vector.

For brevity and simplicity, experiments and specimens belonging to this main series are referred to by their θ value only. Thus, for example, the main series experiment on a specimen with a θ value of 0° is referred to as experiment 0 and the specimen is referred to as specimen 0. This usage is not extended to experiments described below that are extra to the main series (i.e. experiments with equivalent θ values but performed under different conditions). Such experiments are designated, in the text, by No. followed by the sequential number of the experiment.

In order to check the effect of confining pressure on the orientation of a crenulation cleavage or shear band,

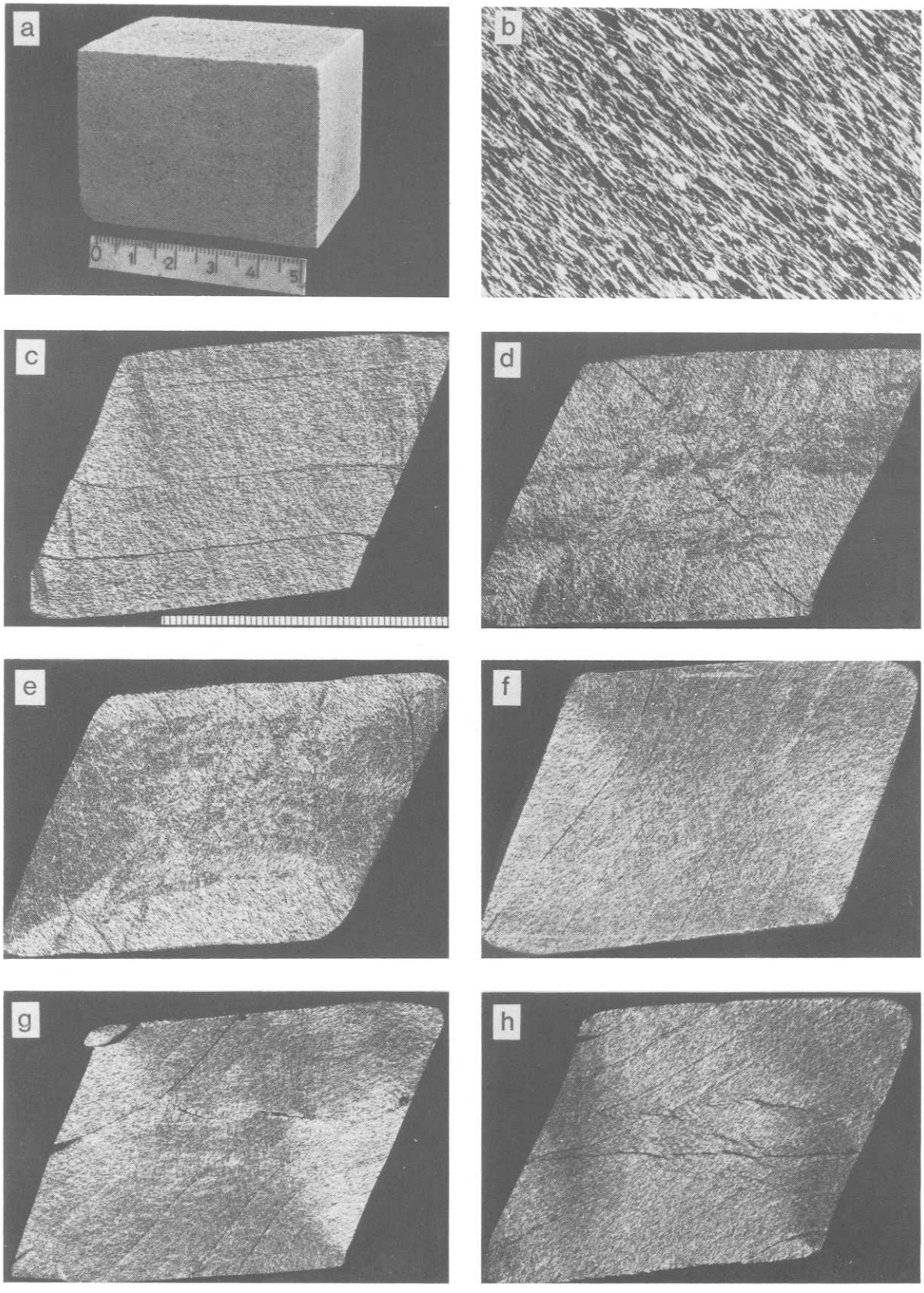

Fig. 1. (a) View of undeformed specimen. (b) Microphotograph of undeformed material showing S_1 foliation composed of mica flakes (white) in salt (black) matrix. Lower edge of photograph is equal to an actual length of 4.2 mm. Crossed polarizers. (c–h) Photomicrographs of thin sections prepared from the mid-plane (normal to the shear plane and parallel to the shear direction) of experimentally deformed blocks of salt–mica schist. Each block has been sheared 30°. Photomicrographs are taken in cross-polarized light. The scale in (c) is mm and applies to all the photomicrographs (c–h). (c) Experiment No. 209, $\theta = 0°$. (d) Experiment No. 212, $\theta = 40°$ conjugate kinkbands. (e) Experiment No. 213, $\theta = 50°$ conjugate kinkbands. (f) Experiment No. 219, $\theta = 110°$ sinistral shear-band cleavage in almost vertical orientation. (g) Experiment No. 221, $\theta = 130°$ conjugate shear-band cleavage approximately symmetrical about S_1. (h) Experiment No. 223, $\theta = 150°$ dextral shear-band cleavage in almost horizontal orientation.

Table 1. Summary of experimental conditions. [a] after an experiment number refers to a second increment of strain on the specimen indicated by the number. θ is initial dip of 'schistosity' (S_1). ϕ is the angular shear strain in degrees and $\dot{\phi}$ is the angular shear strain rate in deg s^{-1}. σ_N is the stress perpendicular to the imposed shear plane in MPa. Mix A is 70 wt % NaCl plus 30 wt % mica and mix B is 70 wt % KCl plus 30 wt % mica. W or D refers to whether the specimen was deformed wet or dry. Asterisks indicate main series experiments

Experiment No.	θ	ϕ	$\dot{\phi}$	σ_N	Mix	W or D
192	150	30	3.3×10^{-4}	20	A	W
195	150	30	3.3×10^{-4}	20	A	W
205	150	30	5.6×10^{-4}	40	B	D
207	150	30	5.6×10^{-4}	10	B	D
208*	20	30	5.6×10^{-4}	20	B	D
209*	0	30	5.6×10^{-4}	20	B	D
210*	10	30	5.6×10^{-4}	20	B	D
211*	30	30	5.6×10^{-4}	20	B	D
212*	40	30	5.6×10^{-4}	20	B	D
213*	50	30	5.6×10^{-4}	20	B	D
214*	60	30	5.6×10^{-4}	20	B	D
215*	70	30	5.6×10^{-4}	20	B	D
216*	80	30	5.6×10^{-4}	20	B	D
217*	90	30	5.6×10^{-4}	20	B	D
218*	100	30	5.6×10^{-4}	20	B	D
219*	110	30	5.6×10^{-4}	20	B	D
220*	120	30	5.6×10^{-4}	20	B	D
221*	130	30	5.6×10^{-4}	20	B	D
222*	140	30	5.6×10^{-4}	20	B	D
223*	150	30	5.6×10^{-4}	20	B	D
224*	160	30	5.6×10^{-4}	20	B	D
225*	170	30	5.6×10^{-4}	20	B	D
226	90	0	0	20	B	D
227	45	0	0	20	B	D
228	0	0	0	20	B	D
229	90	10	5.6×10^{-4}	20	B	D
230	90	20	5.6×10^{-4}	20	B	D
232	50	30	5.6×10^{-4}	20	B	D
232[a]		30	5.6×10^{-4}	20	B	D
233	150	30	5.6×10^{-4}	20	B	D
233[a]		30	5.6×10^{-4}	20	B	D
234	90	30	5.6×10^{-4}	10	B	D
236	150	30	5.6×10^{-4}	80	B	D
237	—	30	5.6×10^{-4}	20	KCl	D

observed in some of the deformed specimens, the experiment for a specimen of $\theta = 150$ (Table 1, experiment No. 223) was repeated at different confining pressures (10, 40 and 80 MPa normal load; Table 1, experiments Nos 207, 205 and 236, respectively). All other conditions were the same as for the main series of experiments.

In order to examine the effects of higher strains on the structures produced, two specimens (Table 1, experiments Nos 232 and 233) were subjected to two increments of 30° angular shear. This was achieved by repeating experiments 50 and 150 and, after the first 30° angular shear, reshaping the deformed specimens into right rectangular prisms by removing a triangular section from one end of each specimen and adding a similar shaped section of new material (with $\theta = 0°$) to the other end. These re-formed specimens were then subjected to another 30° angular shear to produce a total of approximately 50° angular shear.

The conditions for all reported experiments are summarized in Table 1.

RELATIONSHIPS BETWEEN APPLIED FORCES, STRESS AND INITIAL STRAIN

In this section we list the force and displacement data collected from the experiments and discuss aspects of these data that are peculiar to the deformation of strongly anisotropic material in the simple shear rig. This includes a discussion of the conversions of force to stress, stress corrections and the way in which the corrections were determined.

There are three measurements of displacement monitored during each experiment. Shear of the specimen parallel to the shear plane (Fig. 2) is measured by the rotation of the vertical end-faces of the deformation chamber (see Price & Torok 1989). Vertical displacements normal to the shear plane are measured at either end of the lower platen (Fig. 2b). Since this platen is not fully constrained and can tilt up to 5° the vertical displacements are generally unequal and the difference between the two is a measurement of tilt.

Forces are applied to the specimen in two ways (Price & Torok 1989). The platen below the specimen is hydraulically loaded at a pressure that is kept constant (±1 kN) for a given experiment. This tends to shorten the specimen vertically by forcing it against the upper platen which is free to translate horizontally but is fixed vertically. The resulting stress, perpendicular to the shear plane, is referred to as the 'normal stress' and since the specimen is confined on the sides this normal stress consolidates the specimen, both elastically and non-elastically, so that a confining stress is developed around the specimen. The other applied force, referred to as the 'shear force' is that required to rotate the vertical end-faces of the deformation chamber. These rotating end-faces are axial sections cut out of steel shafts which are rotated by a mechanical drive system (see Price & Torok 1989). The shear force is monitored by a remote load cell and is varied during an experiment such that a constant rate of angular shear is maintained.

The relationship between the measured shear force at the load-cell and the shear stress on the specimen varies during an experiment and conversion of the data to stress values is discussed by Price & Torok (1989). The need for a special correction for the materials used in these experiments arises because of their strong anisotropy. The procedure for applying boundary stresses requires that the normal stress be applied before the shear force. In experiments in which the S_1 foliation is inclined to the horizontal shear plane of the rig this normal stress alone is sufficient to cause slip on the inclined S_1 foliation, particularly on the weak bedding planes parallel to S_1 (Fig. 2c). The amount of slippage on S_1 is determined by the slackness of the rig and we observe initial rotations of the vertical end-faces, and of the lower platen of <1.5° (Fig. 3). The torque so induced in the half shafts, forming the end faces, is transmitted to the load-cell as an initial shear force (Figs. 2c and 3). If the slippage induced by the normal stress is dextral then the load-cell measures a negative force and if the slip-

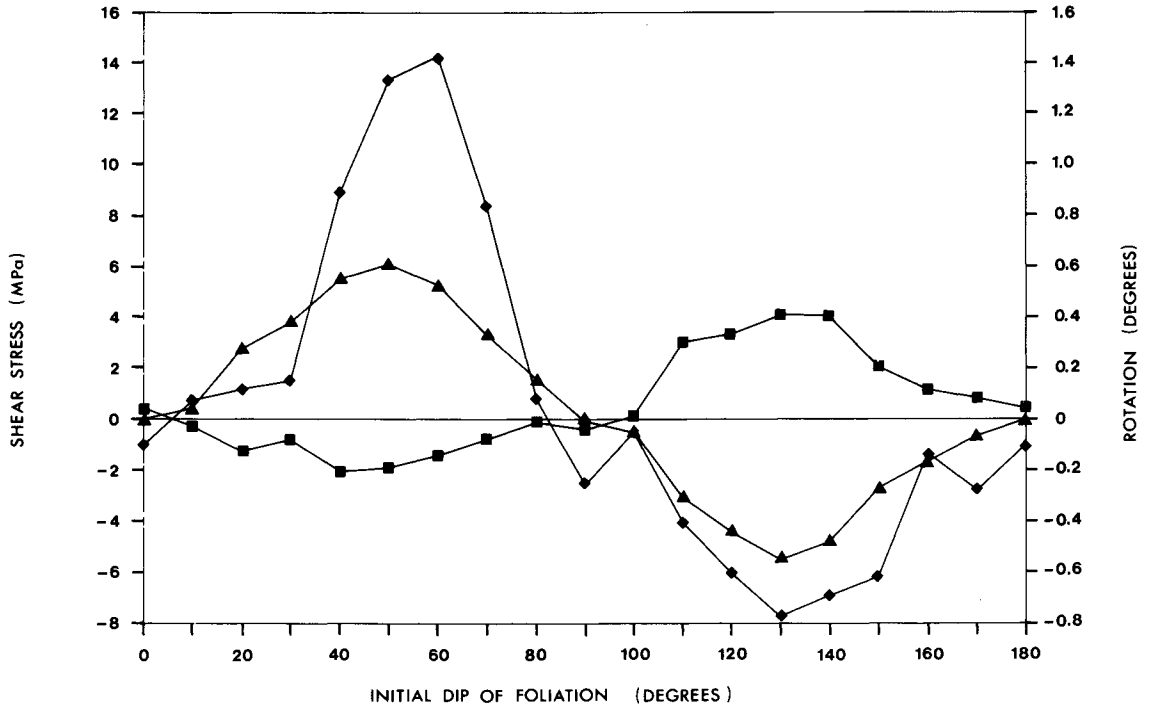

Fig. 3. Graphs of the rotation of the lower platen (diamonds) and the half cylinders (squares) and the initial uncorrected shear stress (triangles) as a function of the initial orientation of S_1 (θ). The graphs represent the conditions prior to the application of the shear force. Negative values are anticlockwise for rotations and dextral for shear stress. See text for further discussion.

page is sinistral the initial shear force is positive (Fig. 3). Where the force is positive it tends to drive the rig in a dextral sense and is therefore simply a component of the shear force and no correction is necessary. Where it is negative the force tends to drive the rig in a sinistral sense and therefore has to be balanced by the applied shear force before a force appropriate to a dextral shear can be generated. Thus the values of shear force measured during the experiment have to be corrected for this initial negative offset.

In addition to the above, the measured forces were corrected for friction in the rig and geometric effects by deforming a block composed of thin Teflon sheets with the sheets aligned parallel to the shear plane. Such a block of separate sheets should have a small initial frictional resistance to shear but should thereafter shear at a constant shear stress. Departure from this constant shear-stress condition represents non-constant conditions in the rig, the major one being an apparent work-hardening due to changing geometry (see Price & Torok 1989). The shear-force–rotation data for the Teflon block was used as a correction curve for data from the salt–mica specimens. Other geometric effects involved in the conversion from shear force to shear stress are described by Price & Torok (1989).

EXPERIMENTALLY PRODUCED STRUCTURES

The structures resulting from the experimental deformation fall into three categories. They are symmetrical folds, kinkbands and shear-band type crenulation cleavage. The first two (Fig. 4) form in specimens with θ values between 10 and 90°, whereas the crenulation cleavage is restricted to specimens with θ values between 110 and 150° (Fig. 5). This natural division of the structures reflects the fact that for experiments with $\theta < 90°$ the S_1 foliation starts in the shortening field of the instantaneous strain ellipsoid whereas for $\theta > 90°$ it starts in, and remains in, the extensional field of the instantaneous strain ellipsoid (Fig. 2b). In the following paragraphs we indicate the more important features observed in specimens 0–90 (Fig. 4).

In specimen 0 the foliation is essentially planar except at the ends of the specimen where it is gently folded or kinked (Fig. 1c). All other specimens display kinkbands and most have a conjugate pair which is best developed in the middle range of θ values (40 and 50°) (Figs. 1d & e). The pair comprises dextral and sinistral members (Fig. 4) which in general lie in appropriate quadrants of the instantaneous strain ellipsoid for the imposed simple shear (Fig. 2b). However, at large θ values (50–90°) the sinistral kinkbands lie in the dextral quadrant (Fig. 4). In specimen 10 and rarely in specimen 20, there is only one member of the conjugate pair, but in addition there is a third group of kinkbands that appear dextral but lie in the sinistral field. Each of the three groups of kinkbands show increasingly clockwise orientations with increasing values of θ. It should be noted that for the purpose of this description we assume that the kinkbands are narrow compared to the domains between them. If this assumption is incorrect a dextral kinkband for example becomes the domain between two sinistral kinkbands.

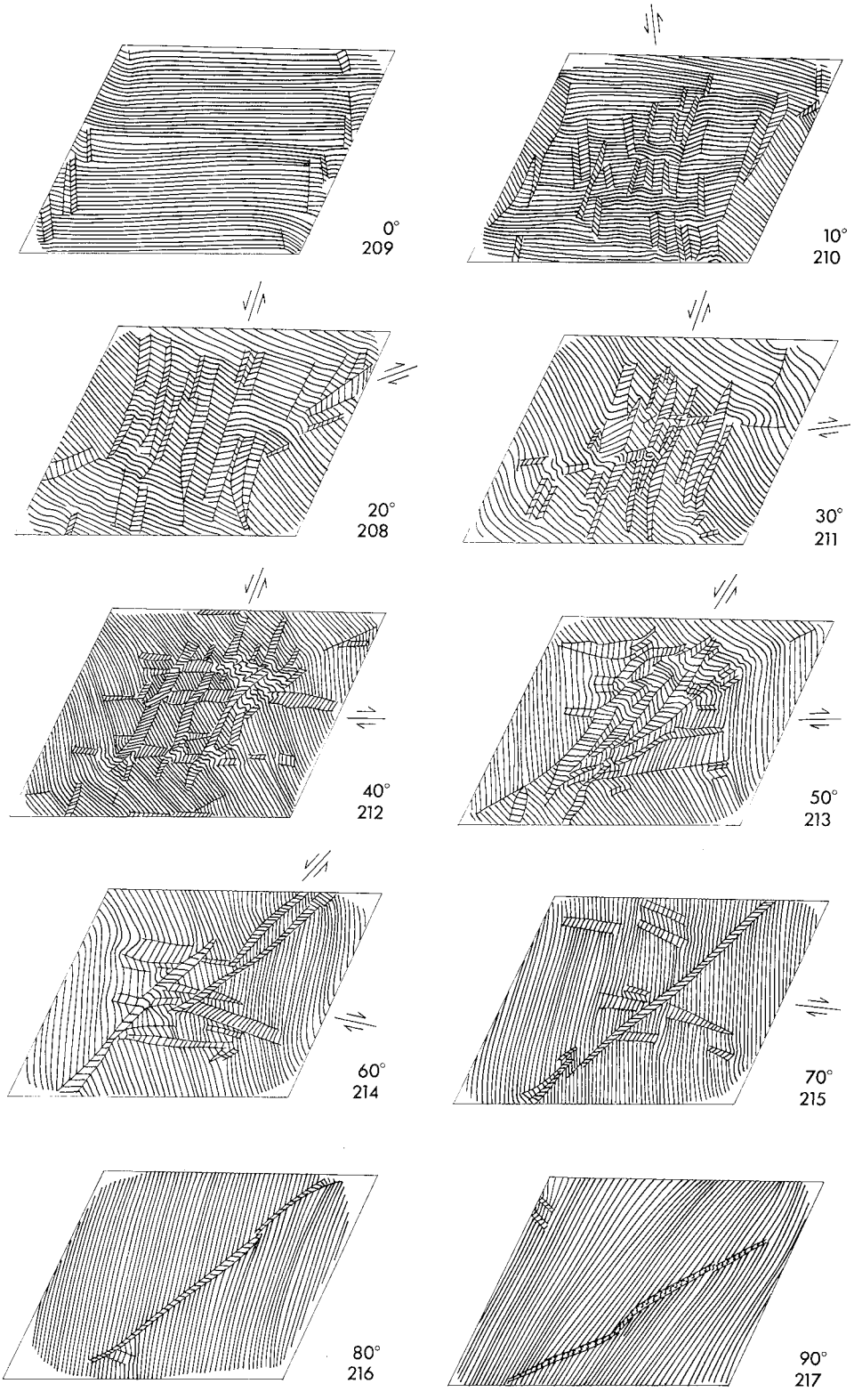

Fig. 4. Sketches of deformed main-series specimens for dips of S_1 (θ) from $\theta = 0°$ to $\theta = 90°$. The first of the two numbers to the right of each sketch is the θ-value and the second is the experiment number (see Table 1).

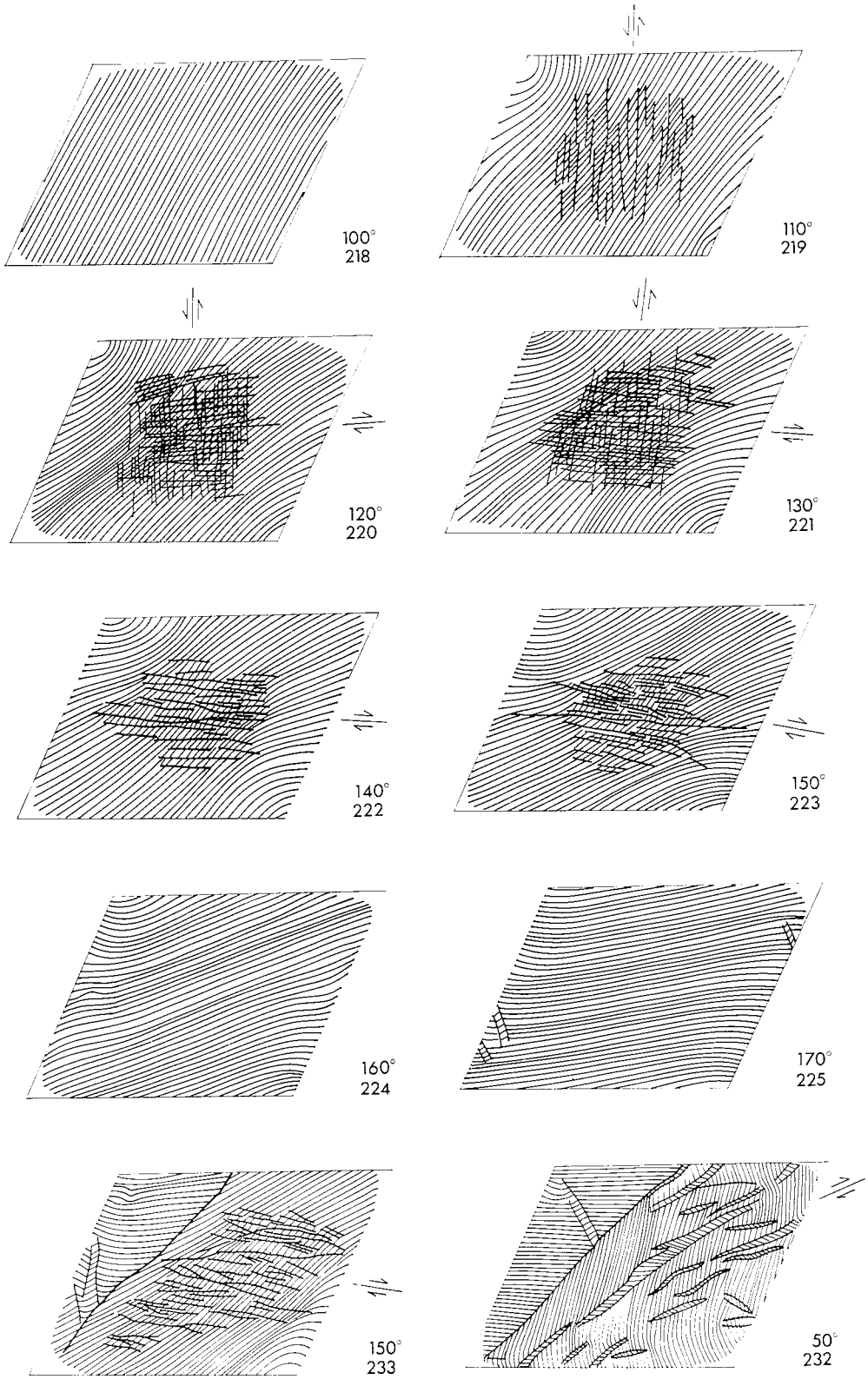

Fig. 5. Sketches of deformed main-series specimens for dips of S_1 (θ) from $\theta = 100°$ to $\theta = 170°$ and large strain specimens for $\theta = 150°$ (No. 233) and $\theta = 50°$ (No. 232). The first of the two numbers to the right of each sketch is the θ-value and the second is the experiment number (see Table 1).

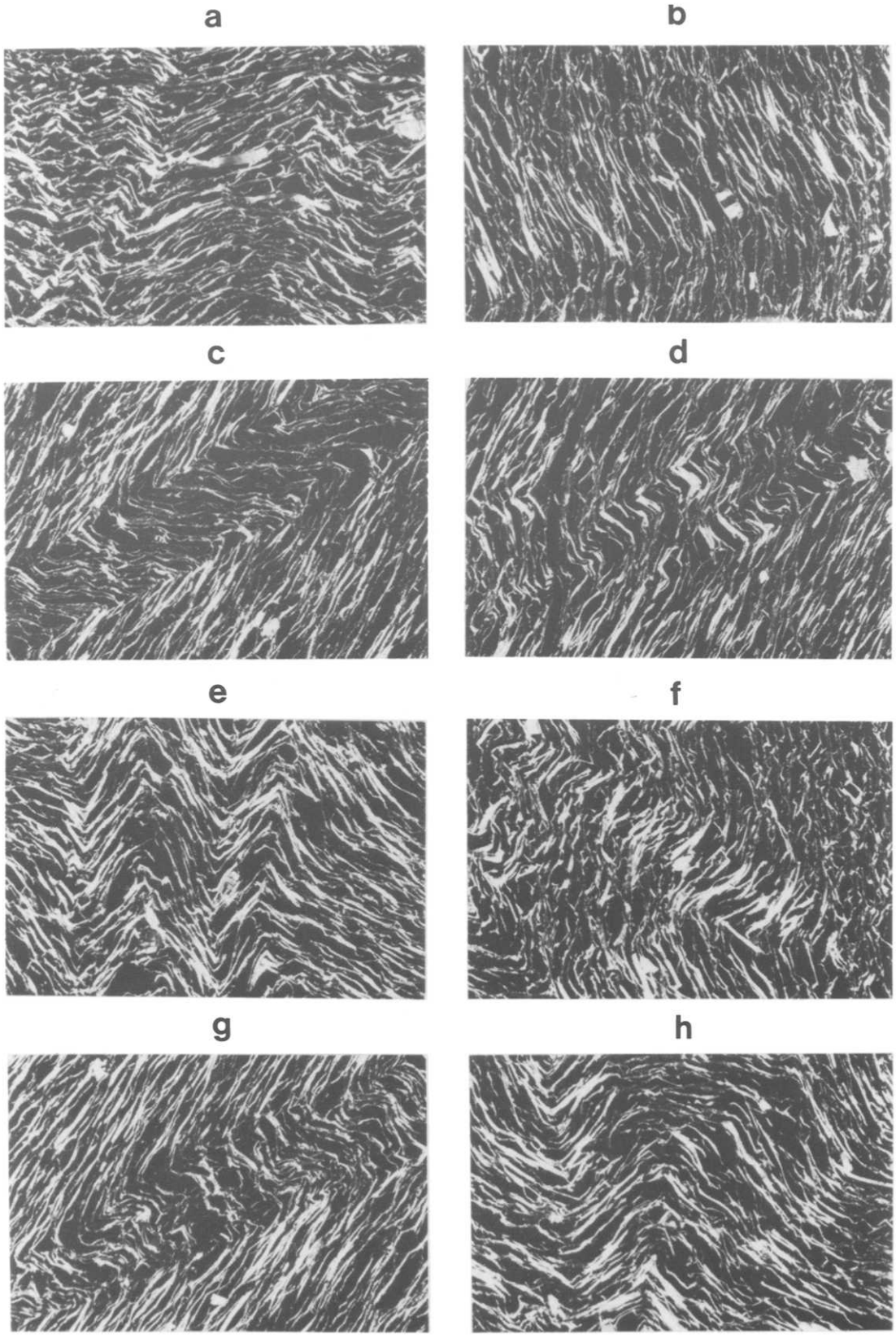

Fig. 6. Microphotographs of kinkbands. Angular shear is 30° for all specimens. For other experimental conditions refer to the appropriate experiment number in Table 1. (a) Broad sinistral kinkband passing through the centre of the photograph; experiment No. 208, $\theta = 20°$. (b) Narrow zone between two dextral kinkbands; experiment No. 215, $\theta = 70°$. (c) Sinistral kinkband; experiment No. 214, $\theta = 60°$. (d) Terminations of adjacent kinkbands that formed during the initial loading normal to the imposed shear plane; experiment No. 217, $\theta = 90°$. (e) Symmetrical kinks; experiment No. 212, $\theta = 40°$. (f) Dextral kinkband; experiment No. 213, $\theta = 50°$. (g) Kinkband due to initial loading of the specimen normal to the imposed shear plane. Note that dextral shear parallel to the initial sinistral kinkband has produced kinks within the kinkband; experiment No. 217, $\theta = 90°$. (h) Intersection of dextral and sinistral kinkbands; experiment No. 213, $\theta = 50°$. All photographs taken with crossed-polarizers. Horizontal edge of photographs is equal to an actual length of 4.2 mm.

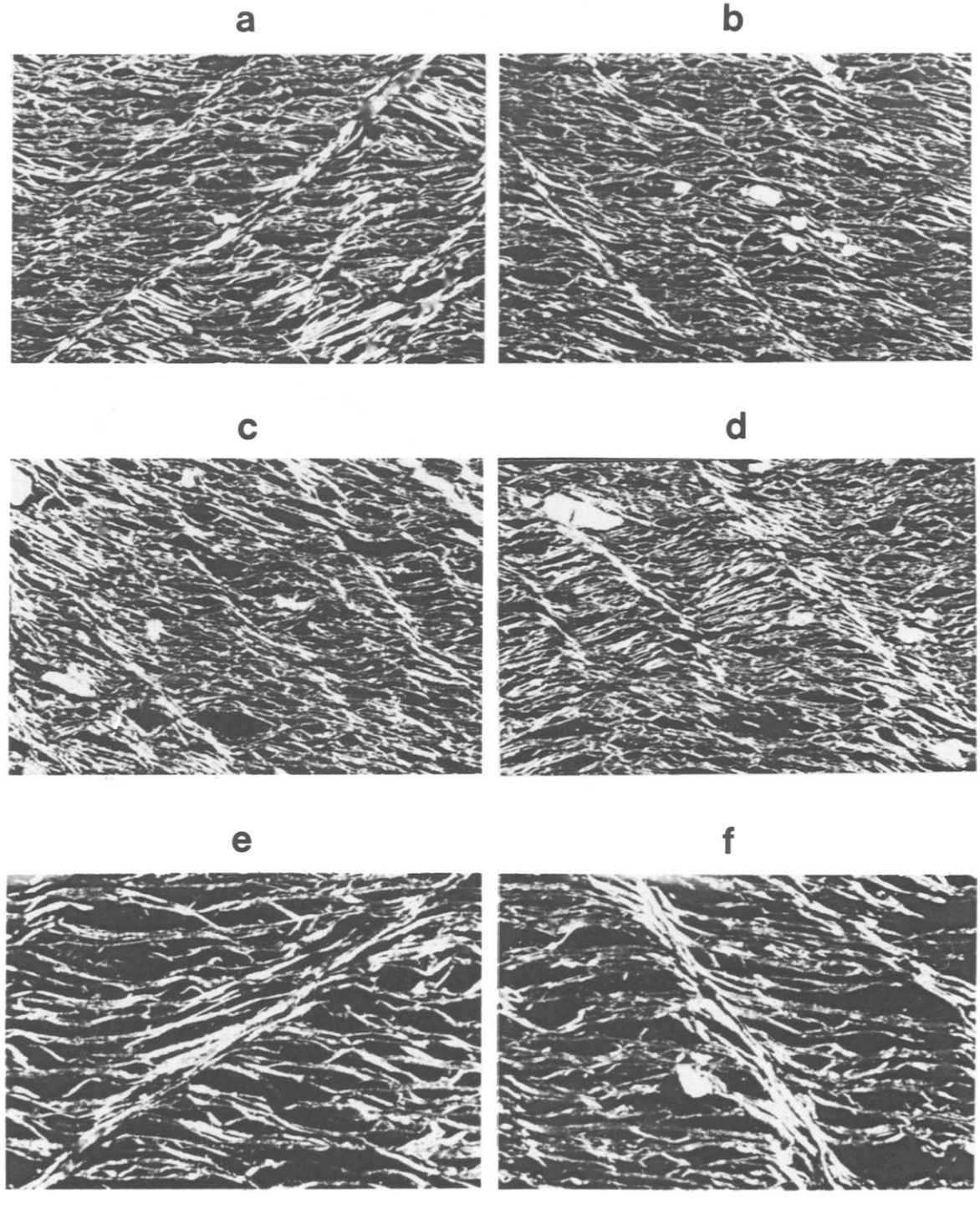

Fig. 7. Microphotographs of shear-band cleavage (S_2). Angular shear is 30° for all specimens. For other experimental conditions refer to the appropriate experiment number in Table 1. (a) Sinistral shear-band cleavage in KCl–mica schist; experiment No. 222, $\theta = 140°$. (b) Dextral shear-band cleavage in KCl–mica schist; experiment No. 222, $\theta = 140°$. (c & d) Shear-band cleavage in 'wet' NaCl–mica schist; (c) experiment No. 195, $\theta = 150°$. (d) experiment No. 192, $\theta = 150°$. (e & f) Detail of individual cleavage (S_2) septae in (e) KCl–mica schist; experiment No. 221, $\theta = 130°$ and (f) 'wet' NaCl–mica schist; experiment No. 195, $\theta = 150°$. Horizontal edge of photographs is equal to an actual length of 4.2 mm for (a–d) and 1.6 mm for (e & f).

The high strain repeat of experiment 50, taken to 50° angular shear strain (Table 1 and Fig. 5, experiment No. 232) produced kinkbands in two dominant orientations similar to those in the less sheared experiment 50. There are differences however: (1) the kinkbands are almost all sinistral despite the fact that they all lie in the dextral field; (2) there is a greater variation in the orientation of the kinkbands in the 50° shear specimen and the mean orientations are rotated clockwise of those in the 30° shear specimen (i.e. specimen 50).

There is a problem in interpretation of kinkbands in specimens with θ values approaching 90° because diagonal kinkbands can develop prior to the start of the shear deformation simply by the application of the normal stress. These kinkbands are not reproducible, being present or absent depending on how tightly the specimen fitted into the deformation chamber. Diagonal kinkbands in specimen 90 (Fig. 4) can be recognized with confidence as structures formed by the normal stress because there is no shortening, only lengthening, of S_1 after commencement of the shear deformation. The problem is not so easily solved for specimens 70 and 80 (Fig. 4). However, there is a change from multiple to essentially single sinistral kinkbands between specimens 60 and 70 (Fig. 4). Consequently we interpret the kinkbands in specimen 60 as a product of the shear deformation and the sinistral kinkbands in specimens 70 and 80 as a product of the normal stress. There are no kinkbands in corresponding specimen 100 but there is a zone of deformed micas that cuts bedding in specimen 110 (Fig. 5) which we interpret as an unfolded kinkband and therefore as a modified product of the normal stress.

Details of the kinkband morphology as seen in thin section are illustrated in Fig. 6. In general the kinkbands are lenticular (Fig. 6d) but some terminate by a broadening of the band and a concomitant decrease in the amplitude of the component kinks. Kinkbands formed at high angle to S_1 comprise open kinks with kinkband boundaries that are not well defined and that are commonly sinuous (Figs. 6a & b). Kinkbands formed at acute angles to S_1 comprise tight kinks with interlimb angles as little as 70° and kinkband boundaries tend to be sharp and straight (Fig. 6c). The angle between S_1 and the kinkband boundary is consistently larger within the kinkband than it is outside the kinkband (cf. Paterson & Weiss 1966). Locally the kinkbands are sufficiently closely spaced to have the appearance of symmetrical kinks (Fig. 6e). Other examples of symmetrical kinks occur at the intersection of conjugate kinkbands (Fig. 6h) similar to those reported by Paterson & Weiss (1966). Kinkbands in specimen 90 (due to normal loading) have a morphology that is distinct from that of all other specimens in that S_1 is kinked within the kinkbands. These second-order kinks are rather irregular but tend to have axial planes inclined to the first-order kinkband boundaries (Fig. 6g). They indicate a reversal in the sense of shear parallel to the kinkband boundary, i.e. the first-order kinkband was sinistral but was later subjected to dextral shear. This is consistent with the extension that occurred parallel to S_1 during this experiment.

Structures observed in specimens 100–170 are represented diagrammatically in Figs. 5 and 7.

There are no new structures developed in specimens 100, 160 and 170 except for localized small folds in the corners of the blocks (Fig. 5). All other specimens have at least one crenulation cleavage (S_2) which is a penetrative feature of the cental region of each specimen (Figs. 1f–h and 5). There is no doubt that these structures are new since they are much more penetrative and persistent than the structures developed during specimen preparation and unlike the latter they cut across 'bedding planes'. These cleavage planes show both dextral and sinistral shear and with respect to shear sense lie in the appropriate field of the instantaneous strain ellipsoid for the imposed simple shear. As with the kinkbands the orientation of each cleavage plane tends to rotate clockwise as θ increases. S_2 is sinistral in specimen 110, dextral in specimens 140 and 150 and occurs as a conjugate pair in specimens 120 and 130 (Fig. 5).

A large strain experiment (Table 1, experiment No. 233) on a replica of specimen 150 produced a very similar S_2 cleavage (Fig. 5). The only significant differences are a slightly more clockwise orientation and a more anastomosing morphology of the cleavage in the high strain experiment.

As seen in thin section (Fig. 7) the S_2 foliation is a normal crenulation cleavage with S_1 preserved in the microlithons and bent around into the S_2 orientation in the septae. Many individual mica grains at the margins of the septae are bent such that they are parallel to both S_1 and S_2 (Figs. 7e & f). Others, lying within the septae, are completely rotated into the S_2 direction. There appears to be an increase in the concentration of mica grains in the septae compared to the microlithons and we assume that this is due to squeezing out of KCl from between the mica grains (cf. Means & Williams 1972). Where 'bedding planes' cross S_2 they can be seen to be displaced distances that are commonly of the same order as the spacing of the S_2 septae. There is no evidence, in the main series of specimens, of brittle failure along the septae that can be said to have developed during deformation (there is local evidence of unloading fractures parallel to S_2). In a repeat (Table 1, experiment No. 207) of experiment 150 run at a lower confining pressure (10 MPa) however, S_2 is less penetrative and is replaced in part by a brittle fault of the same orientation, passing through the centre of the specimen. Repeats (Table 1, experiments Nos 205 and 236) of experiment 150 at higher confining pressures (40 and 80 MPa) gave essentially the same results as experiment 150. The only differences observed are that S_2 is a little weaker, it anastomoses more in the 40 MPa experiment and it dips less steeply (*ca* 15° as opposed to *ca* 20°) in the 80 MPa experiment. We do not know whether these differences are reproducible and therefore whether they are significant or not.

STRESS–STRAIN DATA

Stress–strain data are presented in Figs. 8 and 9. Figure 8 shows curves for the various θ values of the

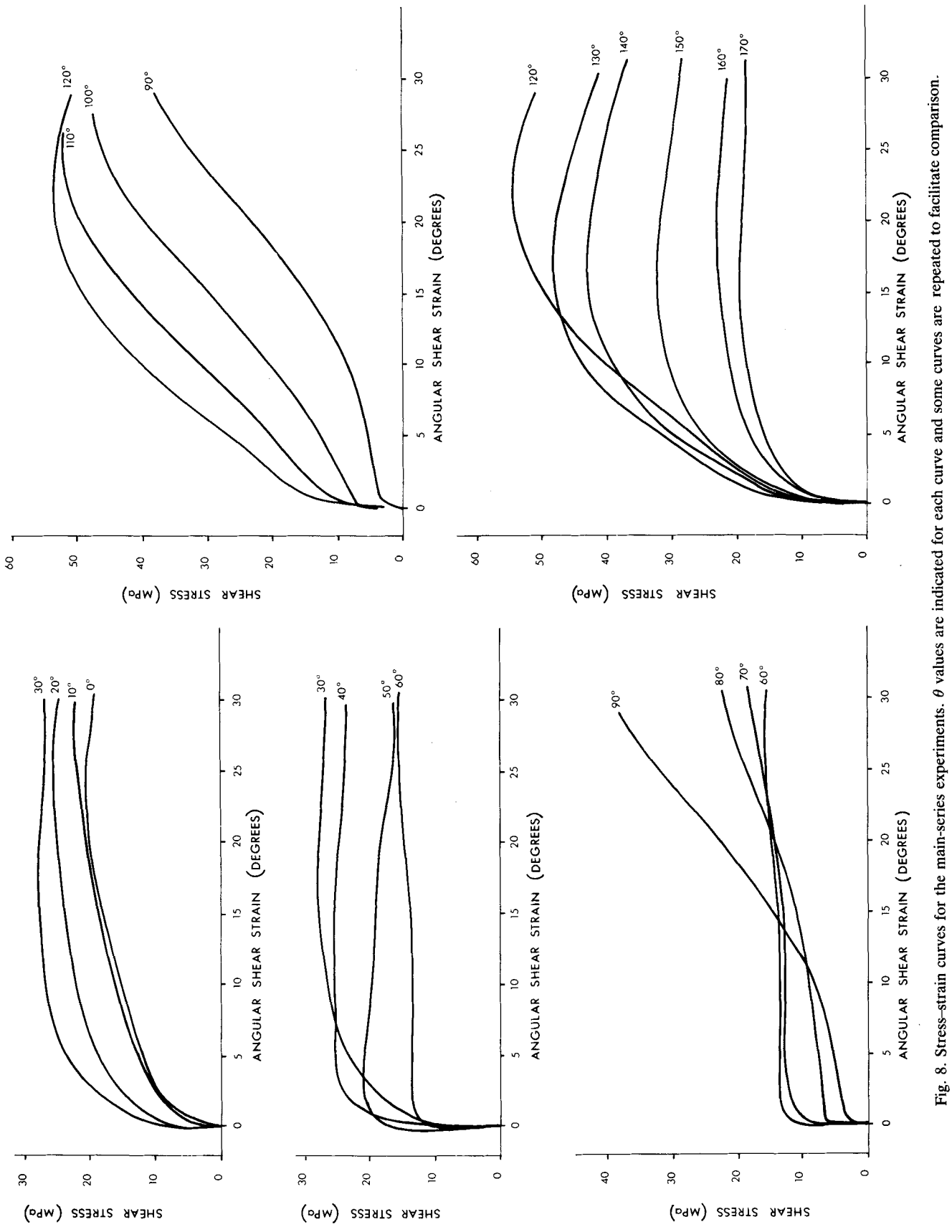

Fig. 8. Stress–strain curves for the main-series experiments. θ values are indicated for each curve and some curves are repeated to facilitate comparison.

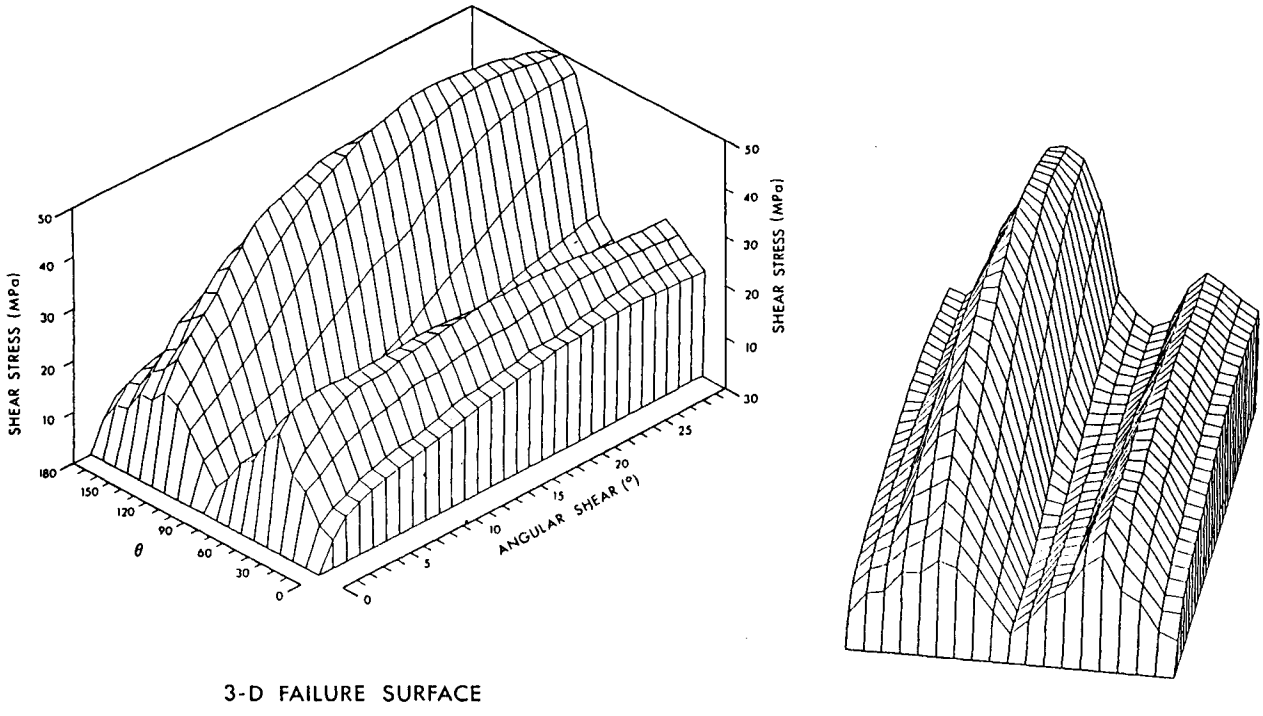

Fig. 9. Two views of the three-dimensional failure surface for the main-series experiments. θ represents the initial dip of S_1 relative to the imposed simple shear plane.

main series of experiments and these curves are combined into a three-dimensional failure-surface in Fig. 9. The graphs of initial flow-strength of the various specimens show fairly symmetrical behaviour, being weak for $\theta = 0°$ and 90° and strong for $\theta = 45°$and 135°.

The work-hardening properties are much less symmetrical (Figs. 8 and 9). Most experiments reach a plateau or maximum in the flow-strength before completion of the experiment at an angular shear strain of 30°. Experiments 70–90 inclusive are the exceptions; they continue to work-harden until the end of the experiment. Maximum flow-strengths increase from experiments 0–30, decrease from experiments 30–60, increase again from experiments 60–120 and finally decrease from experiments 120–170. The lowest flow-strength at an angular shear of 10° is exhibited by experiment 90 and at an angular shear of 30° is exhibited by experiment 60. Experiments 0–50 and 110–170 inclusive all show work-hardening and there is a definite trend for the onset of weakening to occur earlier in each experiment from 10 to 50 and from 110 to 140. Experiment 0 softens earlier than 10 and experiments 150 and 160 soften progressively later than 140, but experiment 170 starts to soften at about the same stage as 140.

Repeats of experiment 150 at different confining pressures behaved predictably for a material deforming at or below the brittle–ductile transition. The greater the confining pressure the greater the strength.

As mentioned above, application of the normal stress results not only in elastic deformation but also, where S_1 is suitably oriented, in slip on S_1. This causes the half-cylinder end-faces and lower platen to rotate before the start of shearing. Another factor contributing to these initial rotations is irregularity in specimen shape. The initial rotations are summarized in Fig. 3 and predictably have maximum values corresponding closely to 45 and 135° and minimum values corresponding closely to 0 and 90°. Neglecting anticlockwise rotations occurring during the initial application of the normal stress, rotations of the platen are all clockwise throughout the experiments except for the calibration experiment with Teflon sheets which shows no significant rotation. This reflects the specimens' tendency to convert Shear Induced Vorticity (SIV) to Spin (see Lister & Williams 1983), a tendency that decreases with increasing planar anisotropy.

DISCUSSION

Deformation mechanisms

The deforming salt–mica 'schist' has various potential mechanisms to achieve the prescribed non-recoverable shape changes. The mechanisms are recognized by the microstructures that they have produced and from the point of view of this study it is useful to classify them as follows.

(1) S_1 *shear.* The material has an initial, strong planar anisotropy and the weakness of specimen 0, the lack of structures in that specimen and the presence of kink-bands in other specimens indicates that shear parallel to that plane has been a significant deformation mechanism. It does not matter from the present point of view whether the shear has been achieved without the loss of continuity or by slip on discontinuities parallel to the foliation. There is however, evidence that both processes have operated. Shear parallel to the foliation

during kinking does not necessarily indicate a perfect simple shearing, the deformation could for example have a component of shortening perpendicular to the shear plane. For the present discussion however, we will use the term 'S_1 shear' with the restricted meaning of a simple shearing parallel to the initial schistosity. If S_1 shear is accompanied by a foliation-normal flattening the flattening is considered here to be an additional mechanism that is described below as 'bulk deformation'.

(2) S_2 *shear.* Some specimens develop new discontinuities (crenulation cleavage or shear bands) that are inclined to the S_1 schistosity, and shear parallel to these discontinuities comprises another deformation mechanism. Again, for the present discussion we consider this mechanism to be a simple shearing parallel to the discontinuities.

(3) *Kinkbands.* The formation of kinkbands is dependent on S_1 shear but it constitutes an independent deformation mechanism since it allows displacements at an angle to the S_1 enveloping surface and therefore behaves like a second slip-system (cf. Paterson 1969). Kinkbands as described here, like any slip system, do not ideally produce an elongation orthogonal with the kinkband boundary. However, slight departures from this condition will result from weak asymmetry of the kinks and in general there will be a slight extension perpendicular to the kinkband boundary.

Once formed the kinks have the potential to tighten by slip on both limbs (as opposed to slip only within the kinkband) and thereby to allow shortening perpendicular to, and extension parallel to the kinkband boundary. Ideally this process should be treated as an additional deformation mechanism. However, it cannot be distinguished with certainty from the other mechanisms and we therefore do not formally treat it as a mechanism.

(4) *Bulk deformation.* There is evidence in some specimens that another mechanism has operated other than the one listed above. This mechanism produces no obvious microstructure as a record of its operation, making its recognition difficult. For example, where there has been shear parallel to S_1, markers parallel to the schistosity in some specimens have moved closer together during deformation, without the development of any new microstructures. In this case we interpret the deformation as an S_1 shearing plus a bulk-deformation. The latter may be a product of crystal-plastic processes or grain-boundary sliding and probably occurred largely in the salt. In nature it could be largely due to solution-transfer processes. The details of the mechanism however, are unimportant. What is important, is that the mechanism allows the 'schist' to deform in ways that are not possible by operation of the other mechanisms.

Timing of kinkband and S_2 *development*

Two of the above mechanisms, kinkband formation and S_2 shear, are dependent on the development of new microstructures and it is important therefore to know when these structures develop. We have no direct knowledge of the magnitudes of angular shear at which they become operative but we do have indirect evidence. Stress–strain curves for specimens in which kinkbands are best developed are characteristically steep at the start and approximately straight and horizontal or gently sloping for most of the experiment (Fig. 8, experiments 40–70). This suggests that the break in slope represents the initial development of kinkbands. Similarly, stress–strain curves for specimens in which S_2 is well developed (Fig. 8, experiments 110–150) are characteristically steep and positive (indicating rapid work-hardening) at the start, rise to a maximum shear stress between 15° and 25° and then gradually pass into a negative slope (indicating work-weakening), and it seems reasonable to interpret the peak as the point at which S_2 shear becomes a significant mechanism.

Explanation of the stress–strain curves

We now analyse the stress–strain data (Figs. 8 and 9) in terms of the deformation mechanisms. Kinkband formation is dependent on S_1 slip so that up to the formation of S_2 all deformation is ultimately dependent on S_1 slip and/or bulk deformation.

As pointed out above the experiments are all conducted close to the brittle–ductile transition and slip will therefore be sensitive to the stress acting normal to the slip-surface. Using engineering terminology (e.g. Hoek & Bray 1977, p. 22), resistance to slip will be a function of the material properties of the slip-plane, viz. cohesion and friction angle, and the component of stress acting normal to the slip-plane (the greater the normal stress the greater the resistance to shear) whereas the driving-force for slip will be resolved shear stress parallel to the slip-plane. The material properties are constants but the magnitudes of the stresses driving and inhibiting the shear (the shear stress and the normal stress acting on the slip-plane) are dependent on the orientation of the slip-plane with respect to the principal stress axes. To a first approximation, since the deformation path is a simple shear, the maximum and minimum principal stress axes will be inclined to the imposed simple shear plane by 45°. Thus the shear stress resolved parallel to the slip-plane (S_1) will be zero when the orientation of S_1 is given by $\theta = 45°$ and 135° and will be at a maximum when $\theta = 0$ and 90°. The normal stress with respect to S_1 will be at a minimum for $\theta = 45°$, at a maximum for $\theta = 135°$ and an intermediate value for $\theta = 0$ and 90°.

We do not have suitable data for determining the friction angle for S_1 at the present time so we can only examine the stress–strain data in qualitative terms. The difference in strength between specimens 40 and 50 and specimens 130 and 140 is qualitatively predictable, in

terms of S_1 slip, since shear stress is equally low in both groups but normal stress is much higher for the second group. The initial weakness of specimens 0 and 90, and continuing weakness of specimen 0 are also explicable since the shear stress is equally high for both and the normal stress equally moderate. What cannot be explained however, in these simple terms, is the fact that specimen 90 yields at a much lower stress than specimen 0. However, at the start of an experiment, as the shear force is applied, there is a transient stage during which the maximum stress axis rotates from an orientation normal to the simple shear plane (where it is after application of the normal force and prior to application of the shear force) to the 45° orientation. During this stage (assuming Poisson's ratio <0.5) the resolved shear stress will be higher and the normal stress lower, with respect to S_1, for experiment 90 than for experiment 0 thus causing specimen 90 to be weaker than specimen 0.

The marked work-hardening of specimen 90 may in part be due to the bulk-deformation mechanism being strong. This mechanism has to be relatively strong or there would be no reason for other mechanisms to develop. The weakest specimens are the ones in which kinkbands are well developed and this may also be explicable in terms of the two stress components. However, there is an additional factor that may contribute to this weakness and that is the fact that kinkband-slip only requires slip on small areas of S_1 and will be localized wherever local deflections in S_1 result in higher than average stress values. Thus the total force required is much smaller than it would be for slip over the whole area of S_1.

In all experiments where S_2 occurs, there is a progressive work-weakening after development of S_2 that continues to the end of the experiment. Further, in all such experiments, once S_2 exists the deformation is presumed to be a combined product of S_1 and S_2 slip, thus it is impossible to say what the strength of the S_2 mechanism is relative to the other slip-mechanisms. However, it is apparently a fairly weak mechanism since it gives rise to work-weakening in experiments that underwent marked work-hardening prior to development of S_2.

Factors influencing the development of kinkbands and S_2

Which of the above mechanisms will operate in a given experiment will be a function of the ease with which the mechanisms are initiated and perpetuated under the prevailing stress conditions. Experiments in which S_1 is parallel to the imposed shear plane are the only ones in which S_1 shear is an adequate mechanism and in all other experiments additional, or other, mechanisms must operate. Kinkbands and S_2 have to develop before they can become viable mechanisms and several factors are involved in their development.

Obviously neither slip-system can develop precisely parallel to S_1 for geometrical reasons. Nor can they develop almost parallel because slip will occur on S_1 before the resolved shear stress on an almost parallel surface can be raised to a high enough value to cause initiation of the new slip surface. The range of values of the angle (α in Figs. 10a & b) between the two, based on empirical observation, is shown in Figs. 10(c) & (d) for both kinkbands and S_2. The minimum value is seen to be large (>35°) suggesting that initiation of kinkbands and S_2 is not just a question of resolved shear stress parallel to the incipient new surface. It may be that the new surfaces can only form parallel to the plane of maximum resolved shear stress when S_1 surfaces have an orientation that will give an appropriate amount of S_1-parallel shortening or extension. Kinkbands can form at all angles between the minimum value of *ca* 40° and almost 90°, but since the kinks are symmetrical the effectiveness of the kinkbands as a slip-system decreases as the angle increases. S_2 surfaces on the other hand have a very restricted range (*ca* 35–45°) in KCl–mica schist (Fig. 10d).

Figure 10(e) shows the constraints, relevant to the formation of a new slip-system, that operate for a foliation (S_1) inclined to the shear plane by 20° (θ = 20°). The circle is divided into dextral and sinistral shear quadrants and the sinistral quadrants are distinguished by the concentric ornamentation. Since the initial foliation lies in the σ_1 quadrant the new slip-surface will be a kinkband (see Fig. 10a); thus Fig. 10(c) showing the possible kinkband orientations with respect to S_1 is superposed on the given S_1 orientation (Fig. 10e). Where a dextral field, with respect to S_1 (stippled area) coincides with a dextral field (unornamented), with respect to stress axes (Fig. 10e), a dextral kinkband could form. The same argument applies to sinistral kinkbands. Thus for the θ = 20° orientation of S_1, both dextral and sinistral kinkbands can form and possible orientations are more restricted for the dextral than for the sinistral kinkbands (Fig. 10e). The heavy lines (Fig. 10e) marked "KB" show the most likely orientations of the kinkbands, at initiation, assuming that they form as near as possible at an angle of 50° to σ_1 (see Paterson & Weiss 1966). The predicted orientations (Fig. 10e) are very close to those observed in the appropriate experiment (Fig. 4, experiment 20).

Figures 10(f) & (g) show all the observed kinkbands and shear-band orientations, respectively, for all of the experiments (all values of θ). It can be seen that all shear-bands lie in the appropriate stress quadrants and the same is true of all dextral kinkbands. Some sinistral kinkbands, however, lie in the dextral stress quadrant but this can be explained by rotation of the kinkbands subsequent to their formation in the sinistral quadrant. The amount of rotation to be expected has been calculated for each 'offending' kinkband, on the assumption that kinkband initiation is marked by cessation of work-hardening. This assumption makes it possible to calculate the amount of strain that occurred after formation of the kinkband and thereby to calculate the amount of rotation that the kinkband underwent. The rotation is sufficient in all cases to return the kinkband to the sinistral quadrant.

A further constraint on the formation of new slip-systems and on the operation of existing systems is that

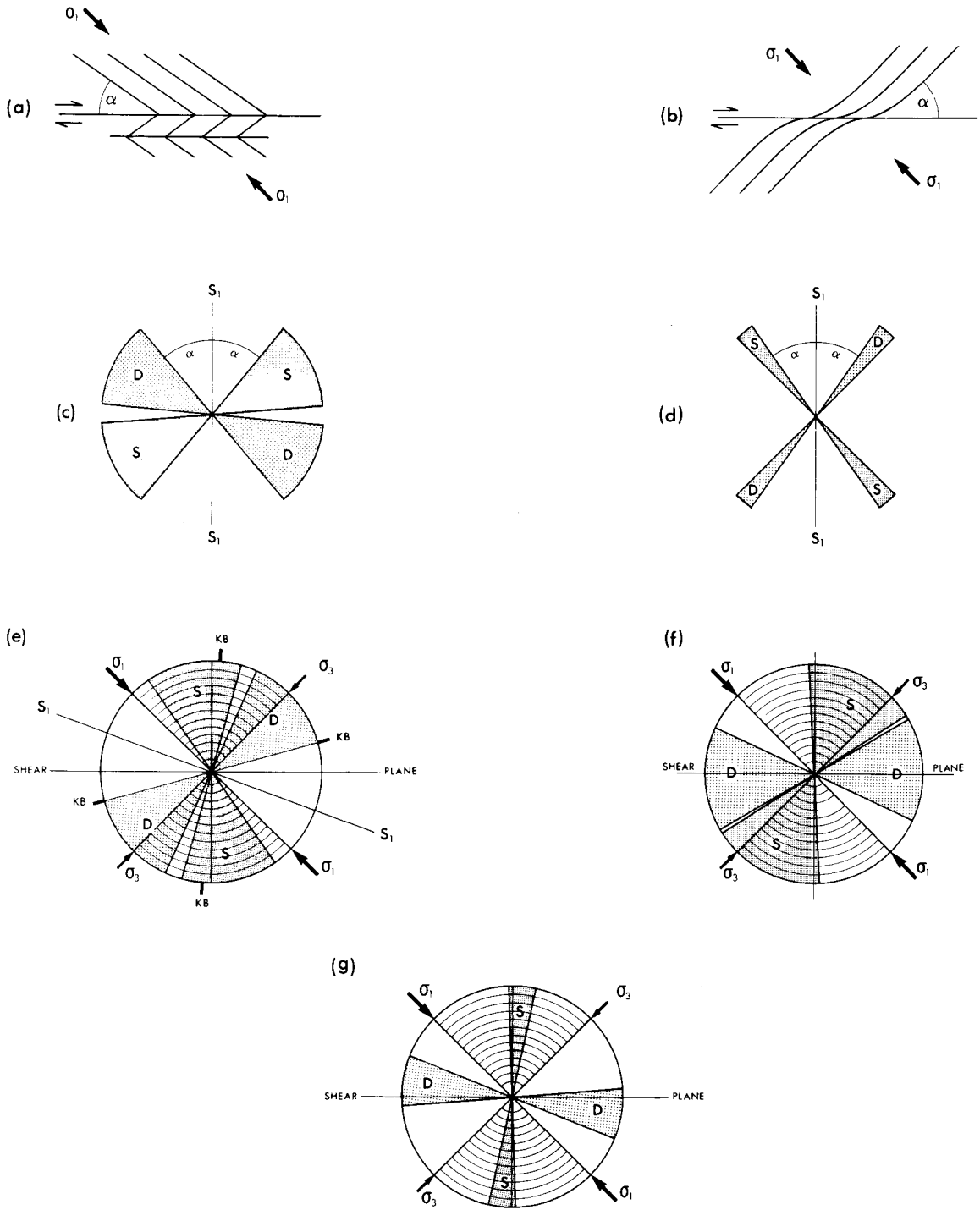

Fig. 10. Summary of constraints imposed by stress and S_1 orientation on the development of kinkbands and shear-band cleavage. See text for explanation. D and S represent fields of dextral and sinistral structures, respectively. Concentric ornamentation (e–g) distinguishes sinistral shear quadrants from dextral shear quadrants (unornamented). (c & d) Possible orientations, with respect to S_1, of kinkbands and shear-band cleavage, respectively. (f & g) Orientation fields (stippled) of all observed kinkbands and shear-band cleavage, respectively.

the systems must be compatible with the imposed strain. This point is demonstrated in Fig. 11 which shows the effect of slip-systems of all orientations on the shape of the specimen as expressed by changes in the length of the two sides AB and BC. If a slip-system, say S_1, lies in a shortening field (1 or 3) with respect to AB, at the start of an experiment while the specimen is still rectangular, it will lie in an extensional field (1 or 3) with respect to BC. Thus operation of the system will shorten AB and lengthen BC. Since the imposed strain path is a simple shearing, AB must remain constant in length and BC must lengthen, thus a second mechanism is needed that will combine with the first to maintain the length of AB while simultaneously lengthening BC. This effect cannot be achieved by a second slip-system at the very start of an experiment, since all orientations of slip-systems

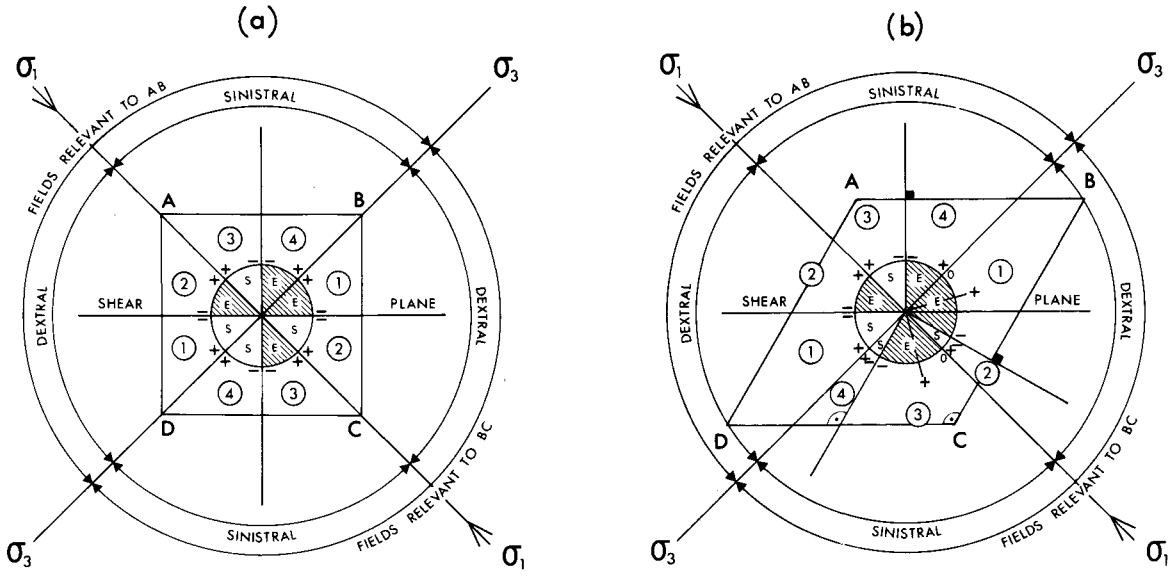

Fig. 11. (a) Diagram showing the relationship of slip-systems (kinkbands and shear-band cleavage) to the stress axes and the effect of their operation on the sides (AB and BC) of the specimen. The diagram is divided into two segments (about the NE axis), one relevant to AB and one relevant to BC. It is further divided into dextral and sinistral quadrants depending on the sense of shear relevant to the slip-plane orientations within each quadrant. The circle within the square is divided into extensional (E) and shortening (S) fields depending on the effect of slip-systems, within each field, on the length of AB and BC. The various fields are numbered 1–4. The positive and negative signs indicate which orientations will have a maximum and a minimum effect, respectively, on the length of AB and BC, for a given shear strain within each field. (b) Diagram showing the effect of strain on the extensional and shortening fields depicted in (a). For further explanation see text.

have the opposite effect on AB to what they have on BC (Fig. 11a). However, once deformation begins and the specimen is no longer rectangular there are orientations of slip-systems that can lengthen AB while lengthening BC (Fig. 11b). If on the other hand, S_1 is so oriented that slip on it causes lengthening of AB then an additional slip-system must develop that shortens AB and lengthens BC.

Thus for simple shear to occur, except in the trivial case where the slip-system is parallel to the imposed shear plane, there must be at least two slip-systems and they must satisfy the following criterion. With respect to AB the slip-systems must lie in both odd and even fields (Fig. 11) and with respect to BC all slip-systems must lie in the odd fields, or if any lie in an even field, they must be so oriented that their effect on BC is small compared to that of the slip-systems in the odd fields (Fig. 11). Any specimen that fails to meet this criterion must deform to a lesser or greater extent by the bulk-deformation mechanism. Further, in so far as the slip-systems are imperfect and give rise to heterogeneous strain all specimens will undergo a certain amount of bulk deformation particularly at their edges.

In summary, we can say that there are constraints on the formation of the slip-systems that have to do with the orientation of the initial foliation and the stress axes (Fig. 10) and further that potentially possible slip-systems will only form and operate if the above criterion is satisfied. Thus we can take, for example Fig. 10(e), which predicts certain orientations for kinkbands, and superpose the predicted orientations on Fig. 11. It can be seen that after a very small amount of strain the dextral kinkbands will be in AB field 1 and BC field 1 whereas the sinistral kinkbands will be in AB field 4 and BC field 3. Thus the criterion is satisfied for deformation by slip on the kinkbands and kinkbands can therefore be expected to form in the predicted orientations and the specimen will be weak. Both predictions are consistent with our observations (see Figs. 4 and 9).

All the experiments have been analysed in the same way and the predictions and observations appear consistent in all cases. Most specimens have sufficient and appropriate slip-systems; those that do not are strong and must have deformed to a large extent by bulk deformation. Why specimens such as specimen 90 do not develop another slip-system remains a question. It may be that the strength of the bulk-deformation mechanism is exceeded before the stress can reach a high enough level parallel to a potential S_2, for S_2 to develop. An alternative possibility is that the formation of S_2 requires the localized rotation of micas away from the preferred orientation of S_1 into the incipient S_2 orientation. Slip on S_1 would inhibit such rotation of mica and might be expected rather to strengthen the S_1 preferred orientation. Thus development of S_2 would be inhibited in specimens, such as specimen 90, in which S_1 shear is strong.

GEOLOGICAL IMPLICATIONS

Our experiments show that very natural-looking kinkbands and shear-band cleavages can be formed in a simple shear where the S_1 foliation is inclined at a suitable angle to the imposed simple shear plane. The same point has been demonstrated experimentally by

Harris & Cobbold (1985) and has been discussed theoretically by Platt (1984), specifically for shear-band cleavage. In our experiments we observe slip parallel to S_1 as well as rotation, as postulated by Platt, and our results and interpretation are therefore in agreement with his analysis. Our results however, indicate that conjugate shear-bands will only form over a limited range of orientations where S_1 is an active surface.

Harris & Cobbold's experiments (1985) with Plasticine are, using our terminology, for initial S_1 orientations of θ = 130, 150 and 165°. In all three experiments they recorded conjugate shear-band cleavages but the surfaces are non-penetrative and their specimens are dominated by anastomosing fracture zones that are approximately parallel to the imposed simple shear plane. Steeply and shallowly dipping shear bands (equivalent to sinistral and dextral shear bands, respectively, in our experiments) are best developed in the 130 and 165° specimens, respectively. There is thus some qualitative similarity between their experiments and ours. However, there are obvious differences; apart from the fact that they have conjugate shear-bands associated with all three θ values, their structures are non-penetrative, and they are dominated by faults parallel to the imposed simple shear plane. Our low confining pressure repeat of experiment 150 is the one that most resembles their specimens and we suggest that the differences may be due to one or more of three factors: (1) more brittle behaviour in their experiments, possibly due to lower confining pressure or faster strain rate; (2) a weaker less penetrative plane of anisotropy; and (3) their experiments allow heterogeneous simple shear whereas ours are constrained to be homogeneous in bulk strain. Harris & Cobbold (1985) suggested that in view of their results care should be exercised in using shear-band cleavage to determine sense of shear. Obviously, where shear-band cleavage occurs in conjugate pairs, unless there is a clear dominance of one pair over the other the structure cannot be used to determine sense of movement. There is no evidence, however, to suggest that where only one penetrative shear-band cleavage exists it can indicate the wrong sense of motion.

Our conclusions, with respect to shear bands, are consistent with the conclusions of Dennis & Secor (1987) and our shear bands are equivalent to their "NSC". They however, do not consider θ values steep enough to give sinistral shear-band cleavage in a dextral shear zone, nor do they consider conjugate shear bands. With respect to kinkbands there is less consistency. Their theoretical analysis only allows for one new slip-plane, their "RSC", which could be equated with our dextral kinkbands. Our results indicate that in the general case there should be two sets of RSC but the analysis remains the same in principle. Their analysis is apparently based on the fact that they only see one orientation of RSC in the field and there is thus a discrepancy not only between our conclusions and their analysis but also between our conclusions and their observations. Two possible explanations can be suggested for the discrepancy with their observations: (1) Dennis & Secor's RSCs are not defined by kinks but by rounded folds that have a much more ductile appearance. It may be that under more ductile conditions conjugate kinkbands are replaced by a single set of folds. This suggestion finds support in coaxial experiments where, as ductility is increased, there is a transition from conjugate kinkbands, symmetrical about the shortening direction, to sinusoidal folds with axial surfaces perpendicular to the shortening direction (Williams & Means 1971); (2) it is possible that the folds of Dennis & Secor formed in what was locally a layer-parallel simple shear environment and that they are drag-folds formed by local conversion of SIV to Spin in the manner suggested by Lister & Williams (1983).

Dennis & Secor (1987) also pointed out that for θ = 0° there should be no new surfaces formed and this conclusion is supported by our experiments. However, in natural shear zones we do see kinkbands and shear-band cleavage developed in S_1 foliations that are parallel or approximately parallel to the margins of the zone and we believe that our experiments demonstrate the significance of this observation as follows.

With respect to the boundaries of the specimens all of the experiments follow simple shear paths. However, strain paths within the specimens, prior to the development of kinkbands and S_2, can be thought of as being partitioned into an S_1-parallel shear component and an S_1-normal shortening or extensional component. This point is demonstrated in Fig. 12(a), where S_1 is assumed to be parallel to EH so that as deformation proceeds slip occurs on S_1 and any given pair of S_1 surfaces move closer together; i.e. the strain-path is 'transpressional' with respect to S_1. The relative magnitudes of the two strain components depend on the orientation of S_1. Thus when S_1 is at 45° to σ_1 the shear component is maximized and the flattening component is zero and when S_1 is at 90° to σ_1 the flattening is maximized and the instantaneous shear is zero. Thus, as discussed above, experiments 10–170 can be thought of as experiments representing simple shear zones in which the S_1 foliation is inclined at various angles to the margins of the zones. Alternatively, they can be thought of as experiments representing small blocks completely contained within 'transtensional' and 'transpressional' shear zones in which S_1 is parallel to the margins of the zones and the ratio of shear to flattening varies with the inclination of S_1 to σ_1 as described above (Fig. 12).

For $0° < \theta < 90°$ the experiments represent transtensional zones (Figs. 12b ii & iii), whereas for $90° < \theta < 180°$ the experiments represent transpressional zones (Figs. 12b v & vi). Thus experiments 70 and 80 represent transtensional zones during the first part of their deformation history and transpressional zones during the second part.

Applying our observations to rocks we therefore conclude that, in shear zones where S_1 is parallel to the zone boundary, the presence of kinkbands indicates that the zone was transtensional (Figs. 12b ii & iii) and the presence of shear-bands indicates that it was transpressional (Figs. 12b v & vi). Conjugate pairs of either structure may form in a shear zone but they indicate that

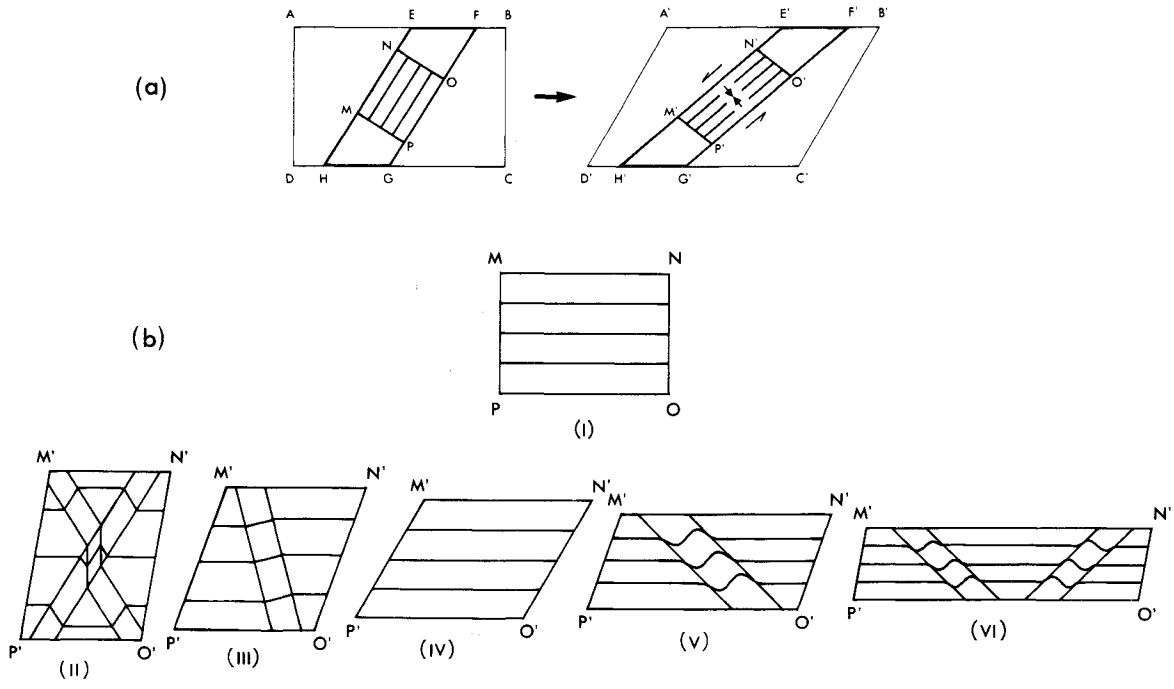

Fig. 12. Partitioning of straining into S_1 parallel shear zones. (a) ABCD represents the experimental specimen. EH is parallel to S_1 and MNOP is a block of material in the centre of the specimen that records the strain history of an S_1 parallel shear zone. By varying the orientation of EH (S_1) the strain history of MNOP can be transpressive (as in the diagram), a simple shear (when EH is parallel to AB) or transtensional (when EH slopes from top left to bottom right). (b) Diagrammatic representation of the structures observed for various ratios of S_1 parallel shear:S_1 normal flattening. (i) Central portion of undeformed specimen (see a); (ii–vi) represent the end results of experiments with different orientations of EH (S_1). In terms of shear zone normal extension or shortening and shear zone parallel shear (ii) represents high extension, low shear; (iii) represents reduced extension and increased shear; (iv) represents no extension and high shear; (v) represents moderate shortening and moderate shear; and (vi) represents high shortening and low shear. See text for further discussion.

the normal component was high relative to the shear component, whereas the presence of a single set of kinkbands or shear-bands indicates that the shear component was relatively high (Fig. 12b). Due to the fact that kinkbands have a greater range of orientations relative to S_1 than do the shear-bands, they are a less sensitive indicator of the ratio of normal strain to shear strain.

Conjugate pairs of shear bands are less commonly reported than single sets and this may be partly due to the fact that they are considered to provide less information about the kinematics of the enclosing shear zones and are therefore of less interest. It is also undoubtedy due in part to the fact that conjugate shear bands are less common. Nevertheless they do occur in many shear zones (e.g. Williams 1967, Platt & Vissers 1980, Behrmann 1987, Marcoux *et al.* 1987) indicating that shear is not always dominant over flattening. The large flattening component may reflect a high volume loss in such shear zones or large flattening strains of the wall rocks during shear. The latter seems a very reasonable explanation for rocks in which ductile shear zones are forming.

It is to be expected that both kinkbands and shear-band cleavage, once formed, will rotate as deformation progresses and our experiments support this supposition. Both structures generally rotate with the same sense of rotation as the sense of vorticity of the experiment. There are however, exceptions, as demonstrated for example by specimen 120 where the SIV (Lister & Williams 1983) associated with the sinistral shear-bands is anticlockwise (despite the overall clockwise vorticity) and this results in an anticlockwise rotation of the weaker dextral shear-bands. Our large strain experiment in the extensional field indicates that as the shear-bands rotate they become more strongly anastomosing (Fig. 5), suggesting that new shear-bands are developing in the favoured orientation as the experiment progresses. The large strain kinkband experiment however, does not show any greater variation in the orientation of the kinkbands (Fig. 5), probably because S_1 was too steep for the formation of new kinkbands after the first strain increment. The specimen does differ from its low strain equivalent however, in that there are no dextral kinkbands, suggesting that they have been unfolded or reversed to produce sinistral kinkbands. What happens to these structures when subjected to still greater shear strains remains a question, but it requires a deformation rig capable of much larger strains than that described here.

In summary we claim that kinkbands will only form in an S_1 if there is an S_1 normal extension and shear-bands will only form in an S_1 if there is an S_1 normal shortening. If there is a sufficiently large S_1 parallel shear component both types of structure will develop as single orientation sets whereas at lower ratios of shear strain to normal

strain they will develop as conjugate pairs. If S_1 is inclined to the boundary of a simple shear zone the structures that develop will depend on local strain partitioning which will be a function of the orientation of S_1 with respect to the boundary-parallel simple shear plane. If S_1 is parallel to the boundary of the shear zone, kinkbands and shear-bands will only develop in zones that are transtensional or transpressional, respectively, and not in simple shear zones. Where only one orientation set is developed, either structure may be used as an indicator of the sense of movement, so long as the geometry coincides with that described here (i.e. the zones have orthorhombic or monoclinic symmetry). We agree with Behrmann's (1987) caution with respect to interpreting shear-band cleavage in zones with triclinic symmetry, however, we do not believe that shear-band cleavage is unreliable in the higher symmetry zones. On the contrary our experiments suggest that it is a very reliable kinematic indicator.

Acknowledgements—We are grateful to Bruce Smith and Peter Torok for excellent laboratory support, Angel Gomez and Mike Thornley for preparation of diagrams and Sherri Townsend for word processing. We are also grateful to Colleen Elliott, Bruce Hobbs, Bruno LaFrance and Chris Mawer for stimulating discussions and constructive reviews. The work was carried out while P. F. Williams held a CSIRO Research Fellowship and this organization is gratefully acknowledged. P. F. Williams also gratefully acknowledges support from NSERC Operating Grant OGP0007419.

REFERENCES

Behrmann, J. H. 1987. A precautionary note on shear bands as kinematic indicators. *J. Struct. Geol.* **9**, 659–666.

Berthé, D., Choukroune, P. & Jegouzo, P. 1979. Orthogneiss, mylonites and non coaxial deformation of granites: the example of the South Armorican shear zone. *J. Struct. Geol.* **1**, 31–42.

Cobbold, P. R., Gapais, D., Means, W. D. & Treagus, S. H. (eds.) 1987. *Shear Criteria in Rocks. J. Struct. Geol.* **9**, 521–778.

Dennis, A. J. & Secor, D. T. 1987. A model for the development of crenulations in shear zones with applications from the Southern Appalachian Piedmont. *J. Struct. Geol.* **9**, 809–817.

Harris, L. B. & Cobbold, P. R. 1985. Development of conjugate shear bands during bulk simple shearing. *J. Struct. Geol.* **7**, 37–44.

Hoek, E. & Bray, J. W. 1977. *Rock Slope Engineering* (2nd edn). Inst. Mining & Metallurgy, London.

Lister, G. S. & Williams, P. F. 1983. The partitioning of deformation in flowing rock masses. *Tectonophysics* **92**, 1–34.

Marcoux, J., Brun, J.-P., Burg, J.-P. & Ricou, L. E. 1987. Shear structures in anhydrite at the base of thrust sheets (Antalya, Southern Turkey). *J. Struct. Geol.* **9**, 555–561.

Means, W. D. & Williams, P. F. 1972. Crenulation cleavage and faulting in an artificial salt–mica schist. *J. Geol.* **80**, 569–591.

Paterson, M. S. 1969. The ductility of rocks. In: *Physics of Strength and Plasticity* (edited by Argon, A. S.). MIT Press, Cambridge, Massachusetts, 377–392.

Paterson, M. S. & Weiss, L. E. 1966. Experimental deformation and folding in phyllite. *Bull. geol. Soc. Am.* **77**, 343–374.

Platt, J. P. 1984. Secondary cleavages in ductile shear zones. *J. Struct. Geol.* **6**, 439–442.

Platt, J. P. & Vissers, R. L. M. 1980. Extensional structures in anisotropic rocks. *J. Struct. Geol.* **2**, 397–410.

Price, G. P. & Torok, P. A. 1989. A new simple shear deformation apparatus for rocks and soils. *Tectonophysics* **158**, 291–309.

Ramsay, J. G. & Graham, R. H. 1970. Strain-variation in shear-belts. *Can. J. Earth Sci.* **7**, 786–813.

White, S. H., Burrows, S. E., Carreras, J., Shaw, M. D. & Humphreys, F. J. 1980. On mylonites in ductile shear zones. *J. Struct. Geol.* **2**, 175–187.

Williams, P. F. 1967. Structural analysis of the Little Broken Hill area of New South Wales. *J. geol. Soc. Aust.* **14**, 317–332.

Williams, P. F. & Means, W. D. 1971. Folding experiments on an artificial schist. *Nature Phys. Sci.* **234**, 90–92.

Williams, P. F. & Zwart, H. J. 1977. A model for the development of the Seve-Koli Caledonian nappe complex. In: *Energetics of Geological Processes* (edited by Saxena, S. K. & Bhattacharji, S.). Springer-Verlag, New York, 169–187.